PAPER

Check for updates

ZnO as a cheap and effective filler for high breakdown strength elastomers†

Liyun Yu [iD] and Anne Ladegaard Skov [iD] *

Cheap, high-performance dielectric elastomers are in high demand from industry concerning new products based on dielectric elastomer transducers. However, formulating an elastomer that fulfils all the requirements for dielectric elastomers is difficult and, first and foremost, not cheap. In this article, we explore the use of a cheap and abundant metal oxide filler, namely ZnO, as a filler in silicone-based dielectric elastomers. The electro-mechanical properties of the elastomer composites are investigated, and their performance is evaluated by means of figures of merit. Various commercial silicone elastomers and a self-formulated silicone elastomer are utilised as elastomer matrices, the effects of which on the final properties of the elastomer composite are investigated.

Introduction

Dielectric elastomers (DEs) are an interesting class of so-called 'stimulus-responsive' polymers on the verge of a commercial breakthrough. Their application possibilities are manifold. When DEs were originally introduced to the research community in the 1990s,[1] they were nicknamed 'artificial muscles', due to their close resemblance performance-wise to human skeletal muscles, and so applications were mainly gathered around this topic.

Various DE-based implants have been developed over the years, such as artificial eyelid controllers[2] and sphincters,[3,4] but it is obvious that DEs are have found broader applications in general, such as in microfluidic flow control,[5] optical lenses,[6] loudspeakers,[7] wave energy harvesters,[8] window frames (haze)[9] and haptics,[10] to mention just a few original ideas for applications currently under investigation.

This broad applicability comes down to some of the main characteristics of dielectric elastomers, namely that they are lightweight, exhibit fast response times (in the order of ms) and are flexible.[11] Another common characteristic of the technology is the perspective of low cost, albeit this is by no means realised as yet, due to the high price of processed thin elastomer films packing the required performance and reliability. Commercial silicone elastomers are available from Wacker Chemie AG in the shape of thin films, but the prices for these films are very high. Thus, currently, the film is only suited for small-volume applications where performance is the competitive factor rather than price. However, Wacker has proven that is possible to produce

thin elastomer films very high in quality, though this does not solve the price issue, for example for large-volume applications such as wave energy harvesting.

At the same time, a substantial amount of research has been conducted into improving further the performance of silicone-based DEs, mainly by improving dielectric permittivity.[12] Various approaches have been utilised and broadly categorised into (1) the addition of high-permittivity solid matter, (2) blending in high-permittivity oils and (3) chemical modification of the silicone backbone with high permittivity moieties.

From a cost perspective category, (3) above is not a feasible path. In general, high-permittivity oils are incompatible with silicone elastomers, and thus category (2) introduces some limitations with respect to ease of processing (and therefore cost) as well as long-term stability.[13–15] This leaves the choice of cheap materials for formulating elastomers with high permittivity matter.

Various fillers have been explored by many different research groups, some examples of which include TiO_2,[16–21] $BaTiO_3$,[22–24] $CuCaTiO_3$,[25–27] carbon nanotubes[28–30] and various other types of conductive carbon structures such as exfoliated graphite[31,32] and functionalised graphene.[33,34]

However, with cheap conductive fillers, potential percolation during processing is a major concern, due to the difficult process of mixing efficiently CNTs, for example, into highly viscous silicone elastomer premixes that will eventually start crosslinking if too much excessive mixing heat is produced. Therefore, formulations for large quantities of a product currently remain limited to various metal oxides.

Metal oxide-filled dielectric elastomers come in a wide range of formulations, ranging from minor additions of silicon dioxide to commercial silicone elastomers (such as Sylgard 184) through to major additions to both commercial[35] and in-lab formulated elastomers. A common problem is that the

Danish Polymer Centre, Department of Chemical and Biochemical Engineering, Technical University of Denmark, Søltofts Plads Building 227, 2800 Kgs. Lyngby, Denmark. E-mail: al@kt.dtu.dk; Fax: +45 45882258; Tel: +45 45252825

addition of fillers in high concentrations is required to achieve significant improvements, but at the same time, the elastomers lose their long-term performance, due to the introduction of various non-elastic phenomena from filler–filler and filler–matrix interactions, such as the Payne and Mullins effect.[13,15,36,37]

In other words, a relatively low degree of networks filling is sought and a low-cost metal oxide such as ZnO should be utilised. Moreover, TiO_2 (as the only cheap Ti-based oxide) does not perform sufficiently well in low enough concentrations to achieve any significant actuation, thereby verifying the additional cost introduced.

ZnO has not been considered in great detail to date, probably due to its relative low dielectric constant ($\varepsilon_r = 8.75$)[38] compared to, for example, TiO_2 (rutile: $\varepsilon_r = 114$, anatase: $\varepsilon_r = 31$), $BaTiO_3$ ($\varepsilon_r = 6000$), copper calcium titanate ($CuCaTiO_3$, CCTO, $\varepsilon_r > 3000$), lead magnesium niobate (($PbMg_{1/3}Nb_{2/3})O_3$, PMN, $\varepsilon_r = 4000$), lead magnesium niobate–lead titanate (($PbMg_{1/3}Nb_{2/3})O_3$–$PbTiO_3$, PMN–PT, $\varepsilon_r = 4000$) and lead zirconia titanate ($PbZrTiO_3$, PZT, $\varepsilon_r = 1800$).[12]

In this study, we investigate dielectric elastomers from a ZnO-silicone elastomer composite (with a low concentration of ZnO) and report an interesting feature of ZnO in the silicone elastomers, namely so-called 'voltage stabilisation'. The same effect has recently been explored through the much more tedious and expensive approach of grafting phenyl groups to the silicone backbone.[39,40]

Experimental

Materials

Two room-temperature vulcanisation (RTV) silicone elastomers (ELASTOSIL® P 7684/60 A/B and ELASTOSIL® RT625 A/B) and one liquid silicone rubber (LSR) (MJK135 4/13 A/B) were provided by Wacker Chemie AG. The mass mixing ratio of premix A and B was 1 : 1 for ELASTOSIL® P 7684/60 and MJK135 4/13, and 9 : 1 for ELASTOSIL® RT625.

Vinyl-terminated PDMS, DMS-V31 ($\bar{M}_n \approx 28\,000$ g mol^{-1}) and a hydride-functional cross-linker, HMS-301, were acquired from Gelest Inc. The platinum cyclovinylmethyl siloxane complex catalyst (511) was purchased from Hanse Chemie, while amorphous silicon dioxide hexamethyldisilazane-treated particles (SIS6962.0) were purchased from Fluorochem.

Two types of zinc oxide nanoparticles (<100 nm particle size, and <50 nm particle size) were acquired from Sigma-Aldrich. Silicone oil (POWERSIL® FLUID TR 50) was provided by Wacker Chemie AG.

Film preparation

0.5, 1.25, 2.5, 3.75 and 5 phr (parts per hundred rubber) of ZnO fillers were mixed into commercial silicone premix A from the respective silicone elastomer, using a FlackTek Inc. DAC 150.1 FVZ-K SpeedMixer™ for 3 minutes at 3500 rpm. Premix B was then mixed into the previous mixture for another 3 minutes at 3500 rpm in the speedmixer.

1.25, 2.5, 3.75 and 5 phr of silicone oil with the same loading of 50 nm ZnO fillers (1.25, 2.5, 3.75 and 5 phr) were mixed into ELASTOSIL® P 7684/60 premix A, using a FlackTek Inc. DAC 150.1 FVZ-K SpeedMixer™ for 3 minutes at 3500 rpm. Premix B was then mixed into the previous mixture for another 3 minutes at 3500 rpm in the speedmixer.

DMS-V31 and 8-functional cross-linker HMS-301 were mixed with treated silica particles (25 wt%) and then mixed by the speedmixer for 3 minutes at 3500 rpm. 0.5, 1.25, 2.5, 3.75 and 5 phr of ZnO fillers and catalyst (511) (1.5 ppm) were then mixed into the previous mixture for another 3 minutes at 3500 rpm in the speedmixer.

The uniform mixtures thus created were coated on a glass substrate using a film applicator (3540 bird, Elcometer, Germany) with a 150 μm blade. The films were cured in an oven for 1 hour at 115 °C, to ensure full curing.

Characterisation

Electrical breakdown strength determination. Electrical breakdown tests were performed on an in-house-built device based on international standards (IEC 60243-1 (1998) and IEC 60243-2 (2001)), and film thicknesses were measured through microscopy of cross-sectional cuts. The distance between the spherical electrodes was set accordingly with a micrometer stage and gauge. An indent of less than 5% of sample thickness was added, to ensure that the spheres were in contact with the sample. The polymer film was slid between the two spherical electrodes (diameter of 20 mm), and the breakdown was measured at the point of contact by applying a stepwise increasing voltage (50–100 V per step) at a rate of 0.5–1 steps per s. Each sample was subjected to 12 breakdown measurements, and an average of these values was given as the breakdown strength of the sample.

Dielectric properties test. Dielectric relaxation spectroscopy (DRS) was performed on a Novocontrol Alpha-A high-performance frequency analyser (Novocontrol Technologies GmbH & Co) operating in the frequency range 10^{-1} to 10^6 Hz at room temperature and at low electrical field (~1 V mm^{-1}). The diameter of the tested 0.5–1 mm thick samples was 25 mm.

Rheological measurements. Rheological characterisation of the prepared films was performed with a TA Instruments 2000 Rheometer set to 2% controlled strain mode, thus helping stay within the linear viscoelastic regime. Measurements were performed with a parallel plate geometry of 25 mm at room temperature, with a normal force of 7 N and in the frequency range 100–0.01 Hz.

Young's modulus and tensile strength measurements. Uniaxial extensional rheology was performed on the series of elastomer films in order to determine the Young's modulus and tensile strength. The stress–strain curves of films were tested at room temperature by ARES-G2 rheometer using the SER2 geometry. A sample of 20 mm length and 6 mm width was placed between two drums and initially separated by a distance of 12.7 mm. The test specimen was elongated uniaxially at steady Hencky strain rate of 0.01 s^{-1} until sample failure at the middle part. Each composition was subjected to four tensile

measurements, which were then averaged. Young's moduli were obtained from the tangent of the stress–strain curves at 5% strain.

Scanning electron microscopy (SEM) and microanalysis. The morphology of the films was investigated with an FEI Quanta 200 ESEM scanning electron microscope, equipped with a field emission gun. The films were coated in 2 nm-thick gold by means of a sputter coater (Cressington, model 208HR) under vacuum condition and a current of 40 mA for 5 seconds. The sample surface was detected with a back-scattered electron detector (BSE) for an incident electron beam of spot 3 accelerated to 15 keV.

The elemental composition of the films was determined by energy dispersive X-rays (EDX) with an Oxford Instruments 80 mm^2 X-Max silicon drift detector Mn Kα resolution at 124 eV. The microanalysis data acquisition and quantification was performed with the Oxford Instruments Aztec program version 3.1.

Fig. 1   The shear modulus as a function of loadings at 2% strain and 0.01 Hz at room temperature for the investigated elastomer composites.

Results and discussion

ZnO particles are not completely compatible with the silicone matrix, as seen in Fig. 1, where most elastomer composites show a clear decrease of the shear modulus with increased loadings of ZnO. Other, larger particles of ZnO were also originally investigated but without any good results due to obvious immiscibility and macroscopic phase separation. For physical compatibility G′ must increase with an increased loading of high modulus particles since physical compatibility requires that the interaction between particles and a network is comparable with that of the crosslinked polymer network. The only elastomer that shows compatibility with the ZnO particles is the RT625 elastomer, which is physically compatible with ZnO particles up to around 2.5 phr. Such a phenomenon may be due to additives within the RT625 elastomer allowing for
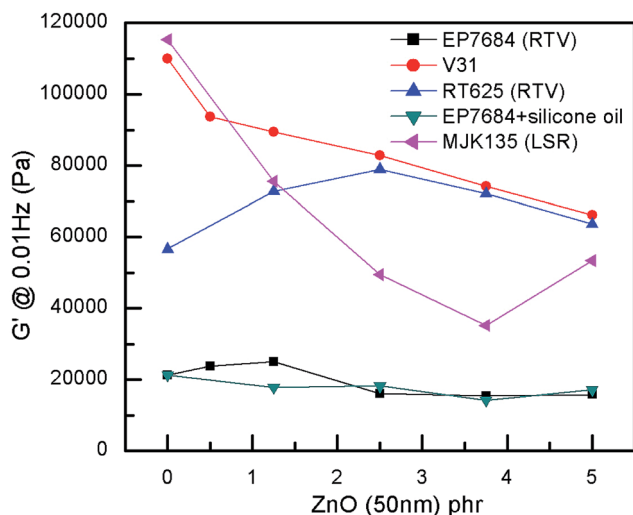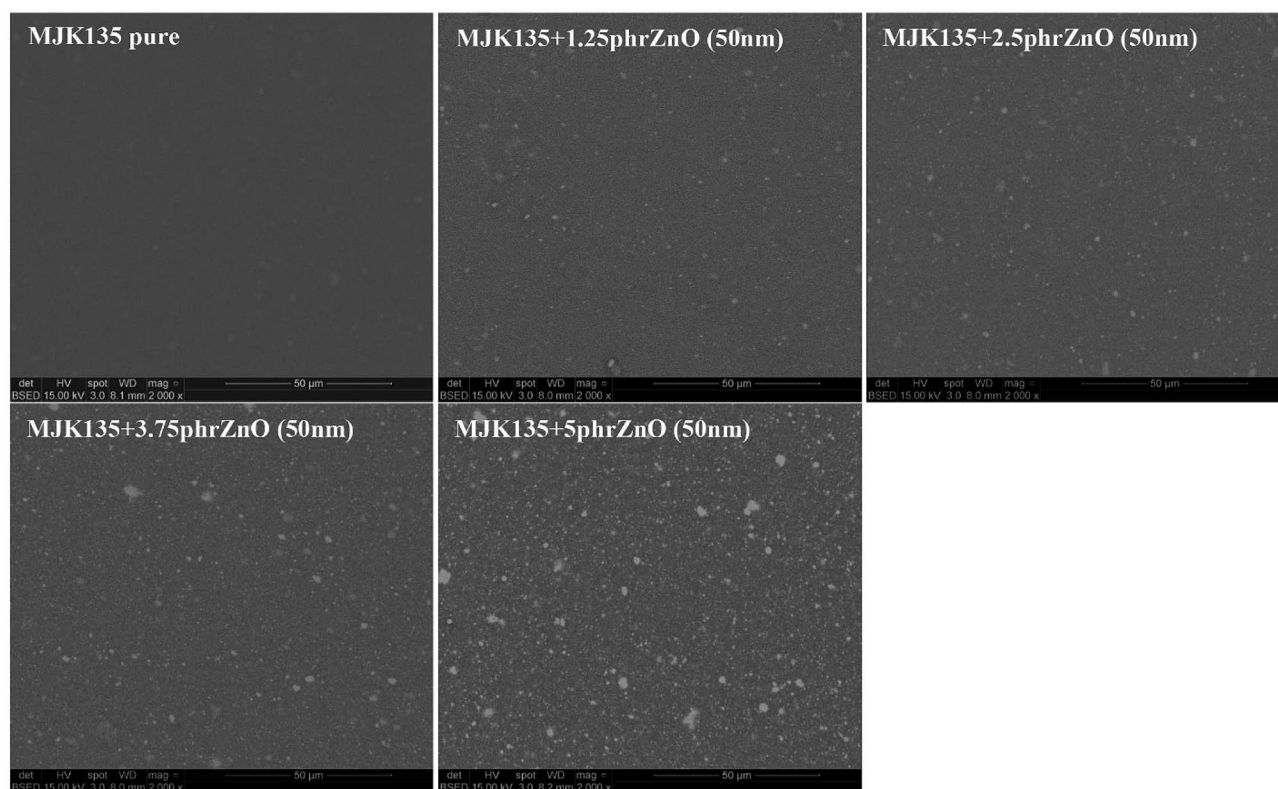

Fig. 2   SEM pictures of the composites from the MJK elastomer with varying loadings of 50 nm ZnO particles.
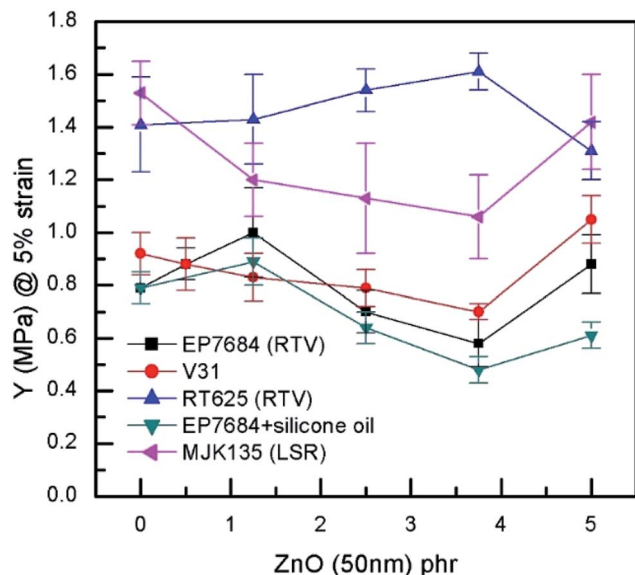
Fig. 4 Young's modulus (@5% strain) as a function of ZnO loading of the investigated elastomer composites at room temperature.

strong physical or chemical interactions between filler and matrix is obvious since there is no significant increase in the Young's modulus with loading. Most of the elastomers increase their Young's modulus for the 5 phr compositions but this is most likely due to percolation of fillers rather than strong filler–matrix interactions. For actuation purposes the overall decrease in Young's modulus is favourable but from a composite perspective it is obvious that the higher loading, the more coherence throughout the matrix. In a similar manner, neither maximum extension nor tensile strength of the composites are strongly influenced by the loading of filler when it is added in minute amounts, as can be seen from Fig. 5.

The dielectric permittivity of the investigated elastomers and the losses, here reported as tan $\delta = \varepsilon''/\varepsilon'$, i.e. dielectric loss relative to dielectric permittivity, are given in Fig. 6. The effect of ZnO on the dielectric permittivity of the resulting elastomer composites is limited when using large amounts of ZnO, due to phase separation, but interestingly, reasonable increases in

dielectric permittivity are identified for loadings up to 5 phr. However, the extent of improvement depends strongly on the type of elastomer matrix utilised in the formulation. The permittivity of the MJK135 formulation remains constant within experimental uncertainty and may be a result of the poor dispersion of ZnO particles within the matrix, as shown in Fig. 2. As an overall conclusion on dielectric permittivity, increases in the range 10 to 35% (compared to the respective reference elastomers) are achieved when excluding the sample showing no improvement. All composites possess very low dielectric losses, generally below 1% except in the case of macroscopic percolation, where it is almost 7%. The latter, however, is still a relatively low dielectric loss.

The electrical breakdown strengths and the Weibull shape parameters of the investigated elastomer composites (shown in Fig. 7) are very promising for some of the formulations, namely the additive-free formulation (V31) and EP7684 without silicone oil. The most remarkable improvement takes place for both composites from 0 to 1.25 phr of ZnO. From the Weibull analysis in Table S3,† it is also obvious that the reliability (as indicated by β) of the films for all EP7684 elastomer composites is decreased compared to the pure elastomer. This indicates that the improvement is a microscopic effect and is sensitive to microscopic inhomogeneities. However, for the additive-free, self-formulated silicone elastomer, it is obvious that the improvement is indeed an overall enhancement, since both electrical breakdown strength (η) and reliability are simultaneously increased. This again confirms earlier observations that the various additives and stabilisers added to commercially available elastomers may determine the degree of improvement by any given method for improving dielectric elastomer properties, and thus one needs to be very careful when formulating elastomers that it is done on the right basis of elastomer. However, the results show that by simple means, such as the addition of minute amounts of ZnO, the electrical breakdown strength as well as the dielectric permittivity can be increased without a significant increase in stiffness to give a rather large overall actuation improvement. This is to be further discussed in the section on figures of merit.

Unsurprisingly, the MJK135 composites show decreased electrical breakdown strengths compared to the pure elastomer,
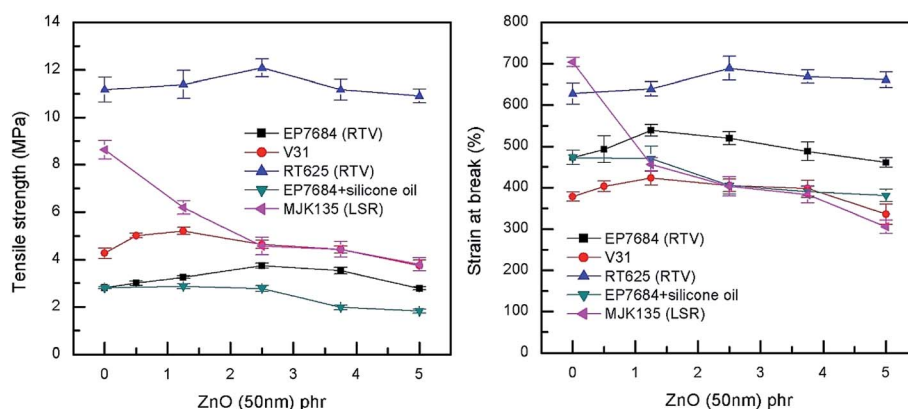

Fig. 5 Tensile strength and strain at break as a function of ZnO loading of the investigated elastomer composites at room temperature.
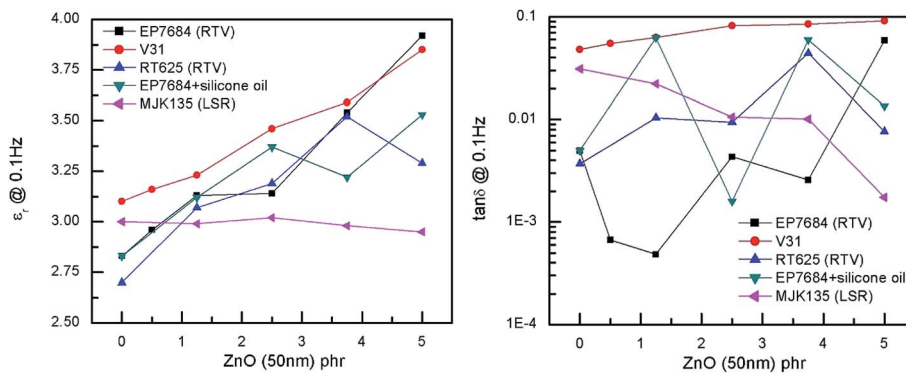
Fig. 6 Dielectric permittivity and dielectric loss (reported as tan δ) as a function of loading of ZnO at room temperature and at a frequency of 0.1 Hz.
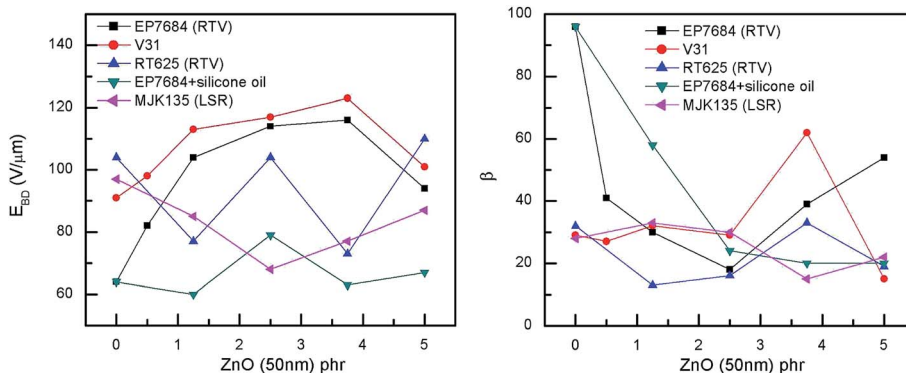

Fig. 7 Electrical breakdown strengths and shape parameter β as a function of ZnO loading of the investigated elastomer composites at room temperature. Weibull statistics for all composites can be seen in Table S3.†
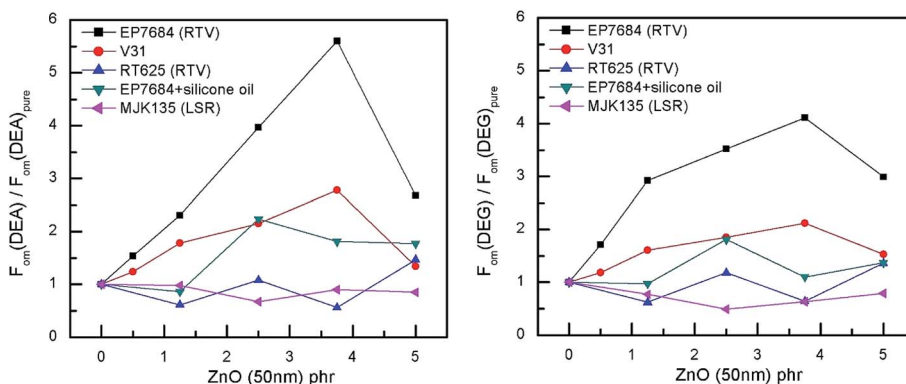

Fig. 8 Figures of merit with respect to actuation (left) and to energy generation (right) for the developed elastomer composites at room temperature. The figures of merit are normalised with respect to the respective pristine elastomers.

as did the RT625 composites. These elastomers were also proven the most inhomogeneous in general. The EP7648 with silicone oil also, to some extent, increased electrical breakdown strengths in line with increased loading, albeit not in a coherent way.

In order to evaluate the overall performance of the developed composites, the respective figures of merits were compared. The figure of merit for actuation is given by:[42]

$$F_{om}(DEA) = \frac{3\varepsilon_r \varepsilon_0 E_{BD}^2}{Y} \qquad (1)$$

where E_{BD} is the electrical field at which electrical breakdown occurs, ε_r is the relative dielectric permittivity, ε_0 is the permittivity of free space (8.85×10^{-12} F m^{-1}) and Y is the Young's modulus of the elastomer.

The figure of merit for energy generation is given by:[43]

$$F_{om}(DEG) = \frac{\varepsilon_r \varepsilon_0 E_{BD}{}^2}{2\Phi} \qquad (2)$$

where Φ is the energy density function of the investigated elastomer. Due to lack of data for most silicone elastomers, it is usually regarded as a constant and is thus ignored in relative comparisons.[12]

The relative figures of merit for the investigated elastomer composites are shown in Fig. 8. In Table S4,† the absolute figures of merit are also shown. Excellent increases in the figures of merit are achieved for the V31 and EP7684 elastomer composites, especially for loadings around 4 phr, where the figures of merit peak. For the best performing composite, namely EP7684 with 3.75 phr loading of ZnO, the figure of merit with respect to actuation was improved by almost a factor of six compared to the pristine silicone elastomer. For the energy generation figure of merit, the improvement was four-fold.

Fortunately, for both systems these elastomer composite films also show great reliability, due to the high β discussed previously. In addition, when not solely discussing performance relative to the pristine elastomer, the EP7684 elastomer composite with 3.75 phr of ZnO transpires as the absolutely best candidate for both actuator and generator material, since the pristine elastomer in itself is a favourable dielectric elastomer candidate.

Conclusions

It was shown that, through the addition of cheap, relatively low dielectric permittivity ZnO particles to pristine silicone elastomers, significant improvements in the actuation and energy generating capabilities of silicone-based dielectric elastomers can be achieved. The improvement partly arises from the so-called voltage stabilization effect. The improvement was verified by means of figures of merit for both actuation and energy generation, as well as a concentration of ZnO of around 4 phr, which was found optimal when considering all relevant aspects. For the best performing elastomer composite, the figure of merit with respect to actuation was improved by almost a factor of six compared to the pristine silicone elastomer. For the energy generation figure of merit, the improvement was four-fold. Higher dielectric permittivities could be achieved by increasing the loading beyond 4 phr, but reliability determined from Weibull analysis on the electrical properties was proven dramatically decreased upon an increased loading above 4 phr. At the same time, it was also proven that there were large variations in improvements, depending on the starting silicone elastomer. Unfortunately, no information on the types and amounts of additives in silicone elastomers is available from elastomer suppliers, and the filler–additive–matrix interactions need to be investigated for each elastomer before knowing the suitability of the given particles to increase the performance of silicone-based elastomer composites. However, it was shown that for a self-formulated silicone elastomer, all interactions were as expected and led to maximum improvements in the dielectric elastomer at relatively low loadings, similar to the commercial elastomer-based silicone composite.

Conflicts of interest

There are no conflicts to declare.

Acknowledgements

References

1 F. Carpi, D. D. Rossi, R. Kornbluh, R. Pelrine and P. Sommer-Larsen, *Dielectric elastomers as electromechanical transducers: fundamentals, materials, devices, models and applications of an emerging electroactive polymer technology*, Elsevier Science, Amsterdam, The Netherlands, 2008, pp. xi.

2 F. Carpi and D. D. Rossi, *Bioinspiration Biomimetics*, 2007, **2**, S50.

3 I. A. Anderson, T. C. H. Tse, T. Inamura, B. M. O'Brien, T. McKay and T. Gisby, *Appl. Phys. Lett.*, 2011, **98**, 123704.

4 V. Leung, E. Fattorini, M. Karapetkova, B. Osmani, T. Töpper, F. Weiss and B. Müller, *Proc. SPIE*, 2016, **9797**, 97970M.

5 D. McCoula, C. Murray, D. D. Carlo and Q. Pei, *Proc. SPIE*, 2013, **8687**, 86872G.

6 L. Maffli, S. Rosset, M. Ghilardi, F. Carpi and H. Shea, *Adv. Funct. Mater.*, 2015, **25**, 1656.

7 R. Heydt, R. Kornbluh, J. Eckerle and R. Pelrine, *Proc. SPIE*, 2006, **6168**, 61681M.

8 R. D. Kornbluh, R. Pelrine, H. Prahlad, A. Wong-Foy, B. McCoy, S. Kim, J. Eckerle and T. Low, *Proc. SPIE*, 2011, **7976**, 797605.

9 S. Shian and D. R. Clarke, *Soft Matter*, 2016, **12**, 3137.

10 F. Carpi, S. Bauer and D. D. Rossi, *Science*, 2010, **330**, 1759.

11 P. Brochu and Q. Pei, *Macromol. Rapid Commun.*, 2010, **31**, 10.

12 F. B. Madsen, A. E. Daugaard, S. Hvilsted and A. L. Skov, *Macromol. Rapid Commun.*, 2016, **37**, 378.

13 S. B. Zakaria, F. B. Madsen and A. L. Skov, *Polym.-Plast. Technol. Eng.*, 2017, **56**, 83.

14 F. B. Madsen, S. B. Zakaria, L. Yu and A. L. Skov, *Adv. Eng. Mater.*, 2016, **18**, 1154.

15 S. B. Zakaria, L. Yu, G. Kofod and A. L. Skov, *Mater. Today Commun.*, 2015, **4**, 204.

16 F. Carpi and D. D. Rossi, *IEEE Trans. Dielectr. Electr. Insul.*, 2005, **12**, 835.

17 H. Liu, L. Zhang, D. Yang, Y. Yu, L. Yao and M. Tian, *Soft Matter*, 2013, **11**, 363.

18 M. Cazacu, M. Ignat, C. Racles, M. Cristea, V. Musteata, D. Ovezea and D. Lipcinski, *J. Compos. Mater.s*, 2014, **48**, 1533.

19 M. Razzaghi Kashani, S. Javadi and N. Gharavi, *Smart Mater. Struct.*, 2010, **19**, 035019.

20 S. Javadi and M. Razzaghi-Kashani, *Proc. SPIE*, 2010, **7642**, 76421E.

21 S. Vudayagiri, S. B. Zakaria, L. Yu, S. S. Hassouneh, M. Benslimane and A. L. Skov, *Smart Mater. Struct.*, 2014, **23**, 105017.

22 H. Zhao, L. Zhang, M. Yang, Z. Dang and J. Bai, *Appl. Phys. Lett.*, 2015, **106**, 092904.

23 D. Khastgir and K. Adachi, *J. Polym. Sci., Part B: Polym. Phys.*, 1999, **37**, 3065.

24 H. Böse, D. Uhl, K. Flittner and H. Schlaak, *Proc. SPIE*, 2011, **7976**, 79762J.

25 L. J. Romasanta, P. Leret, L. Casaban, M. Hernández, M. A. de la Rubia, J. F. Fernández, J. M. Kenny, M. A. Lopez-Manchado and R. Verdejo, *J. Mater. Chem.*, 2012, **22**, 24705.

26 S. Vudayagiri, S. Zakaria, L. Yu, S. S. Hassouneh, M. Benslimane and A. L. Skov, *Smart Mater. Struct.*, 2014, **23**, 105017.

27 G. L. Wang, Y. Y. Zhang, L. Duan, K. H. Ding, Z. F. Wang and M. Zhang, *J. Appl. Polym. Sci.*, 2015, **132**, 42613.

28 S. K. Yadav, I. J. Kim, H. J. Kim, J. Kim, S. M. Hong and C. M. Koo, *J. Mater. Chem. C*, 2013, **1**, 5463.

29 K. Goswami, A. E. Daugaard and A. L. Skov, *RSC Adv.*, 2015, **5**, 12792.

30 S. S. Hassouneh, L. Yu, A. L. Skov and A. E. Daugaard, *J. Appl. Polym. Sci.*, 2017, **134**, 44767.

31 M. Tian, Z. Wei, X. Zan, L. Zhang, J. Zhang, Q. Ma, N. Ning and T. Nishi, *Compos. Sci. Technol.*, 2014, **99**, 37.

32 S. S. Hassouneh, A. E. Daugaard and A. L. Skov, *Macromol. Mater. Eng.*, 2015, **300**, 542.

33 L. J. Romasanta, M. Hernández, M. A. López-Manchado and R. Verdejo, *Nanoscale Res. Lett.*, 2011, **6**, 508.

34 J. Zhang, S. Liang, L. Yu, A. L. Skov, H. M. Etmimi, P. E. Mallon, A. Adronov and M. A. Brook, *J. Polym. Sci., Part A: Polym. Chem.*, 2016, **54**, 2379.

35 S. C. Shit and P. Shah, *Natl. Acad. Sci. Lett.*, 2013, **36**, 355.

36 J. Diani, B. Fayolle and P. Gilormini, *Eur. Polym. J.*, 2009, **45**, 601.

37 S. Cantournet, R. Desmorat and J. Besson, *Int. J. Solids Struct.*, 2009, **46**, 2255.

38 C. Jagadish and S. J. Pearton, *Zinc oxide bulk, thin films and nanostructures: processing, properties, and applications*, Elsevier Science, Amsterdam, The Netherlands, 2011, p. 407.

39 A. H. A Razak and A. L. Skov, *RSC Adv.*, 2017, **7**, 468.

40 A. H. A Razak, L. Yu and A. L. Skov, *RSC Adv.*, 2017, **7**, 17848.

41 A. L. Larsen, P. Sommer-Larsen and O. Hassager, *Proc. SPIE*, 2004, **5385**, 108.

42 P. Sommer-Larsen and A. L. Larsen, *Proc. SPIE*, 2004, **5385**, 68.

43 T. G. McKay, E. Calius and I. A. Anderson, *Proc. SPIE*, 2009, **7287**, 72870P.